SSRG International Journal of Mechanical Engineering
ISSN: 2348-8360/ https://doi.org/10.14445/23488360/IJME-V13I8P104

Volume 13 Issue 8, 33-42, August 2026
© 2026 Seventh Sense Research Group®

Original Article

Effect of Laser Cladding Parameters on the Surface Roughness of Stellite 6 Coatings on Cylindrical AISI 1045 Steel

Nguyen Van Cuong[1], Toan Thang Le[1,2]*, Thu Quy Le[2]

[1] *Faculty of Mechanical Engineering, University of Transport and Communications, Hanoi, Vietnam.*
[2] *National Research Institute of Mechanical Engineering, Hanoi, Vietnam.*

**Corresponding Author : thanglt@utc.edu.vn*

Received: 08 June 2026 Revised: 29 July 2026 Accepted: 12 August 2026 Published: 27 August 2026

Abstract - *This study investigates the influence of laser cladding parameters on Surface Roughness (Rz) of Stellite 6 coatings on cylindrical shaft substrate of AISI 1045 steel using Taguchi L9 orthogonal array with three replications. Stellite 6 powders were deposited on AISI 1045 steel substrate using the laser cladding method with laser power, scanning speed, powder feed rate, and overlap ratio as input parameters. Surface topography was measured using a 3D non-contact optical microscope. The Analysis of Variance (ANOVA) and quadratic regression modeling were performed based on experimental results. Experimental Rz values were varied between 30.09 and 66.44 µm. ANOVA showed that the overlap ratio was the dominant factor affecting the surface roughness, followed by scanning speed and powder feed rate, while laser power had a significant non-linear effect on roughness. A statistically significant quadratic regression model ($F = 63.83$, $p < 0.001$) was developed to predict Rz response. According to the regression model and main effects plots, optimum laser power of 1800 W, scanning speed of 800 mm/min, powder feed rate of 15 g/min, and overlap ratio of 60% were predicted to achieve the minimum value of Rz. The predicted minimum value of Rz from the regression model was found to be 18.11 µm. Confirmation experiment was conducted at the predicted optimum setting, which resulted in an average Rz of 19.55 µm, revealing a prediction error of 7.4%. Therefore, increasing the overlap ratio improves surface uniformity and reduces the post-machining allowance required for laser-clad shaft components.*

Keywords - *Laser cladding, Stellite 6, Surface roughness, Taguchi method, ANOVA, Regression model.*

1. Introduction

Laser deposition is a surface coating process in which the coating metal and a thin layer of substrate are melted by a focused laser beam to form a metallurgically bonded coating. Compared with conventional welding-based deposition processes, laser cladding provides more localized heat input, a relatively narrow heat-affected zone, and better control of coating dilution [1, 2]. However, the quality of the cladding layer remains sensitive to processing conditions. Laser power and scanning speed determine the amount of energy delivered to the substrate, while the powder feed rate affects the balance between the supplied material and the melt pool's melting capacity.

In multi-track cladding, the overlap ratio introduces an additional thermal and geometrical effect because every new track partially remelts the preceding one [3-5]. Stellite 6 is a Co-Cr-W-C alloy commonly selected for components subjected to combined wear, corrosion, and elevated-temperature exposure. Its performance is associated with a cobalt-rich matrix strengthened by chromium- and tungsten-containing carbides [2, 6]. Laser-clad Stellite 6 has therefore been studied on different ferrous substrates, including AISI 1045 steel, cast iron, and stainless steel. Most published work has concentrated on microstructure, dilution, hardness, wear, and corrosion behavior. Several authors, such as [7], examined the tribological behavior of laser-clad Stellite 6 on steel substrates, including AISI 1045 steel, while authors in [8] studied the influence of laser power on the microstructural and mechanical properties of coaxially deposited Stellite 6 coatings.

The surface roughness of a multi-track coating depends not only on the roughness of each bead but also on how successive beads are superimposed. Ocelík et al. showed that the geometry of an overlapped coating can be related to the shape of a single track and the distance between adjacent tracks [9]. Chen et al. subsequently developed and experimentally assessed a geometrical model for the surface smoothness of multi-track laser-clad layers [10]. These studies indicate that an unsuitable track offset leaves pronounced valleys or causes excessive local material accumulation, even

This is an open access article under the CC BY-NC-ND license (http://creativecommons.org/licenses/by-nc-nd/4.0/)

when the individual tracks are deposited without obvious defects. Experimental studies have also demonstrated the importance of the overlap ratio.

Tanigawa et al. reported that increasing laser-path overlap reduced the surface roughness of multi-track layers by decreasing the height difference between neighboring tracks [11]. Zareh and Urbanic found that variations in overlap percentage changed the geometry and continuity of single-layer multi-track deposits [12].

However, the effect of increasing overlap is not independent of the other processing variables. Additional overlap increases the amount of remelting and changes the local thermal history; its effect may therefore depend on laser power, scanning speed, and powder supply.

Several previous studies have focused on hardness, microstructure, and wear performance [13-17], while the influence of laser coating parameters on the surface roughness Rz of Stellite 6 coatings deposited on cylindrical AISI 1045 steel substrates has received less attention. Previous work by the authors evaluated the mechanical properties and corrosion resistance of Stellite 6 deposited on flat AISI 1045 specimens using a single processing condition, without considering surface roughness [18].

In contrast, the present study examines the Rz roughness of Stellite 6 coatings on cylindrical shafts. Studies on multi-track surface formation have mainly used flat substrates or other material systems.

The effects of laser power, scanning speed, powder feed rate, and overlap ratio on the Rz roughness of Stellite 6 coatings deposited on cylindrical AISI 1045 steel remain insufficiently understood. Therefore, this study focuses on the effects of laser cladding parameters on the surface roughness of Stellite 6 coatings deposited on cylindrical AISI 1045 steel shafts using a Taguchi L9 experimental design.

2. Materials and Methods

2.1. Materials

Medium-carbon steel AISI 1045 was chosen as substrate material due to its extensive application to shaft-type parts such as transmission shafts, pump shafts, piston rods, and rotating parts that work under moderate mechanical loads. The base material consisted of cylindrical bars with a Diameter (D) of 80 mm and a Length (L) of 500 mm.

AISI 1045 steel contains around 0.45 wt.% carbon, providing good strength, hardness, toughness, and machinability. For these reasons, AISI 1045 was selected as a representative engineering material for components operating under combined mechanical loading and corrosive environments.

The substrate surfaces were turned before laser cladding to provide a uniform surface finish, degreased using acetone and dried using warm air flow to remove impurities and ensure stable metallurgical bonding between substrate and coating.

The coating material consisted of Stellite 6 alloy powder, a cobalt-based alloy of chromium, tungsten, and carbon. Stellite 6 exhibits high resistance to wear, oxidation, and corrosion in the presence of chloride ions. Such excellent performance can be attributed to hard chromium-rich carbides uniformly dispersed in the cobalt-rich Face-Centered Cubic (FCC) matrix [2, 8].

The average powder particle size was approximately 50 μm. The powder particles were dried at 120 °C for 30 min before deposition to remove absorbed moisture and enhance feeding stability. Nominal chemical compositions of substrate and cladding powder materials are shown in Table 1.

Table 1. Nominal chemical composition of the substrate and cladding powder (wt.%).

Element	**Co**	**C**	**Si**	**Fe**	**Cr**	**Mn**	**Mo**	**W**
Stellite 6	Bal	1.1	1.0	1.5	28.5	1	1.2	4.2
Element	**Fe**	**C**	**Si**	**Mn**	**Cr**	**Ni**	**P**	**S**
AISI1045 Steel	Bal	0.45	0.36	0.5	0.25	≤0.2	≤0.04	≤0.04

2.2. Experimental Procedure

The laser cladding experiments were carried out by a 6kW fiber laser source (Raycus RFL- C6000) coupled to a four-axis CNC machine. The Stellite 6 powder was supplied coaxially through the melt pool from a rotary disk powder feeder, while high-purity argon gas was used as the carrier gas and shielding gas to prevent oxidation during processing. The substrate for coating deposition was a cylindrical AISI 1045 steel shaft with 80 mm diameter (Figure 1).

Prior to the cladding experiments, substrate surfaces were turned and then cleaned with acetone and dried. The Taguchi method was used to study the influence of four main process parameters, such as laser Power (P), Scanning Speed (Vs), Powder Feed Rate (Mp) and Overlap Ratio (O), on the quality of coating produced. The design matrix consisted of three levels of four factors, which were presented according to the L9 orthogonal array listed in Table 2.

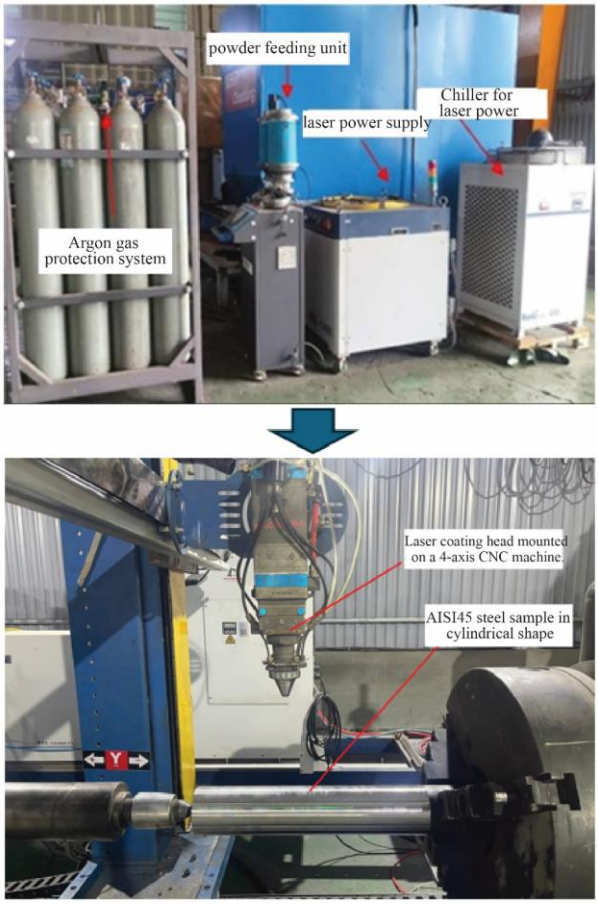

Fig. 1 Experimental setup of the laser cladding system

Table 2. The parameters of the laser cladding process

Exp. No.	Laser Power, P (W)	Scanning Speed, Vs (mm/min)	Powder Feed Rate, Mp (g/min)	Overlap Ratio, O (%)
1	1800	600	12	40
2	1800	700	15	50
3	1800	800	18	60
4	2000	600	15	60
5	2000	700	18	40
6	2000	800	12	50
7	2200	600	18	50
8	2200	700	12	60
9	2200	800	15	40

Photos of nine specimens coated with Stellite 6 that were made on C45 steel shafts are presented in Figure 2 based on the Taguchi L9 array experiment design. It is clearly seen that specimens exhibit differences in appearance. This indicates that variations in the laser cladding parameters affected surface morphology and roughness of coatings. To evaluate the individual effects of the selected process parameters, all other processing conditions were kept constant throughout the experiments.

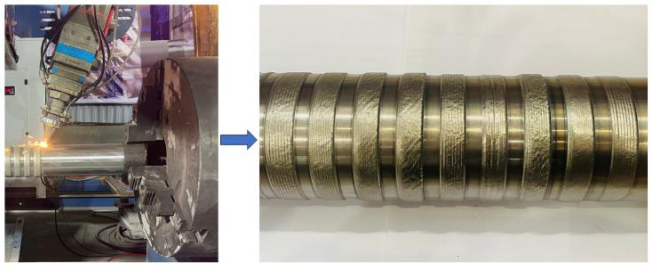

Fig. 2 Stellite 6-coated samples from the Taguchi L9 design

Surface topography was characterized using an Olympus DSX1000 non-contact optical measuring system employing focus-variation technology. The system reconstructs a three-dimensional surface profile by acquiring a stack of images at different focal positions along the Z-axis in accordance with ASME B46.1 [19] and ISO 4287 [20]. The Olympus DSX1000 system was calibrated according to the manufacturer's recommended procedure before each measurement session. Surface roughness was measured at three different locations on each specimen, and the average value was used for subsequent analysis.

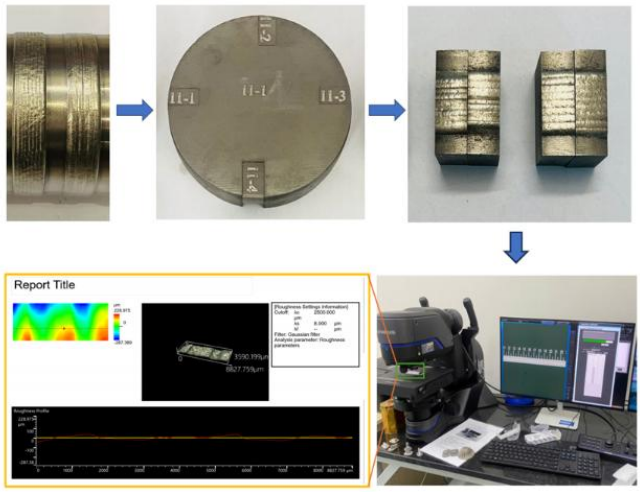

Fig. 3 Sample preparation and surface roughness measurement procedure

Since the coated specimens were in the form of cylindrical shafts (ϕ80 mm), each shaft was cut into rings before being cut into three segments equally spaced around the circumference of the shaft. Specimens were acetone cleaned and dried before measurements were taken, and were never ground or polished to maintain as- cladded condition of the specimen surfaces.

Three representative regions of each coating condition were taken along the axial direction of the shaft, and the average Rz was used as the final value of the surface roughness measurement. Figure 3 shows the procedure used for specimen preparation for surface roughness measurements.

The laser-cladded shaft was cut into rings, then each ring was cut into three representative segments. The as-cladded surfaces were analyzed with an Olympus DSX1000 3D optical microscope to measure the Rz roughness parameter.

3. Results and Discussion

3.1. Cross-Sectional Morphology of the Coatings

Table 3 presents the cross-sectional morphologies of the nine investigated Stellite 6 coatings prepared under different processing parameters defined by the Taguchi L9 design. All cross-sections revealed continuous coatings with sound metallurgical bonding to the C45 substrate, suggesting that all parameter combinations allowed for enough melting of powder particles and bonding to the substrate.

Table 3. The parameters of the laser cladding process

No	Cross-Sectional Morphology of the Coatings
1	
2	
3	
4	
5	
6	
7	
8	
9	

There are visible differences between the cross-sections regarding coating geometry and surface profile. Samples 1, 5, and 9 feature large waviness between neighboring clad tracks and large valleys (small overlap) while the surface was poorly leveled. Tracks of samples 2, 6, and 7 had higher overlap, and the coating thickness was more uniform, but the local surface still featured irregularities. Samples 3, 4, and 8 seem to have the smoothest cross-sectional morphology as coating thickness remained stable while neighboring tracks featured stable overlap and flat top surfaces.

No cracking or severe bonding defects were present in any sample cross-section. Only a few isolated pores are visible in some samples, but their amount is low enough not to influence coating properties. It can be concluded that the greater overlap ratio led to more uniform coatings and improved surface morphology. Samples 3, 4, and 8 showed the most homogeneous cross-section among all tested conditions.

3.2. Surface Roughness Results

The Surface Roughness (Rz) of the laser-cladded Stellite 6 coatings is presented in Table 4. Surface roughness was measured at three different locations on each specimen (Rz1, Rz2, and Rz3), and the average value was used for subsequent analysis. The average Rz values ranged from 30.09 to 66.44 μm, indicating that the surface morphology was strongly influenced by the laser cladding parameters.

The Standard Deviation (SD) of the three measurements ranged from 1.88 to 4.46 μm, corresponding to approximately 2.8-11.3% of the average Rz values. Compared with the corresponding average Rz values, these deviations were relatively small, indicating good repeatability of the surface roughness measurements and satisfactory consistency of the measurement procedure.

Table 4. Experimental results of surface roughness Rz

ExpNo.	P (W)	Vs (mm/min)	Mp (g/min)	O (%)	Rz1 (μm)	Rz2 (μm)	Rz3 (μm)	Average Rz (μm)	SD (μm)
1	1800	600	12	40	58.13	52.74	53.25	54.71	2.98
2	1800	700	15	50	40.92	44.78	47.48	44.39	3.30
3	1800	800	18	60	30.22	29.57	33.82	31.20	2.29
4	2000	600	15	60	36.11	33.06	41.09	36.75	4.05
5	2000	700	18	40	65.41	68.61	65.30	66.44	1.88
6	2000	800	12	50	63.54	58.98	63.09	61.87	2.51
7	2200	600	18	50	63.24	61.96	65.86	63.69	1.99
8	2200	700	12	60	30.89	32.85	26.55	30.09	3.22
9	2200	800	15	40	45.49	40.67	36.59	40.92	4.46

To facilitate regression modeling and evaluate the influence of processing parameters on the Surface Roughness Response (Rz), the input variables were transformed from their actual values into coded variables. Parameter coding eliminates differences in units and value ranges among the factors, thereby improving the stability and reliability of the statistical analysis.

Four processing parameters, including laser Power (P), Scanning Speed (Vs), Powder Feed Rate (Mp) and Overlap Ratio (O), were investigated in this work. The variables were coded as X_1, X_2, X_3, and X_4, respectively based on equation

$$X_i = \frac{Z_i - Z_{0i}}{\Delta Z_i} \quad (1)$$

where X_i is the coded value of the i^{th} parameter, Z_i is the actual value of the parameter, Z_{0i} is the center-point value, and ΔZ_i is the step interval between adjacent levels.

Three coding levels (-1, 0, and +1) were assigned to the low, center, and high levels of each factor, respectively. Accordingly, the coded variables were defined as:

$$X_1 = \frac{P-2000}{200} \quad (2)$$

$$X_2 = \frac{V_s-700}{100} \quad (3)$$

$$X_3 = \frac{M_p-15}{3} \quad (4)$$

$$X_4 = \frac{O-50}{10} \quad (5)$$

The coded experimental matrix was subsequently used to develop the regression model and to statistically evaluate the effects of laser cladding parameters on the Surface Roughness (Rz) of the Stellite 6 coatings.

3.3. Analysis of Variance (ANOVA)

The ANOVA results obtained using the coded variables are presented in Table 5. The developed quadratic regression model was highly significant, with an F-value of 63.83 and a p-value of < 0.001, indicating that the selected process parameters significantly affected the surface roughness of the laser-clad Stellite 6 coatings.

Table 5. ANOVA results for the surface roughness Rz.

Source	DF	Adj SS	Adj MS	F-Value	P-Value
Regression	8	4847.02	605.88	63.83	0.000
X_1	1	9.66	9.66	1.02	0.327
X_2	1	223.80	223.80	23.58	0.000
X_3	1	107.40	107.40	11.31	0.003
X_4	1	2049.22	2049.22	215.88	0.000
X_1^2	1	706.81	706.81	74.46	0.000
X_2^2	1	8.85	8.85	0.93	0.347

X_3^2	1	680.34	680.34	71.67	0.000
X_4^2	1	1060.94	1060.94	111.77	0.000
Error	18	170.86	9.49	-	-
Total	26	5017.88	-	-	-

Among the linear terms, the overlap ratio (X_4) exhibited the strongest influence on surface roughness, with an F-value of 215.88 ($p < 0.001$). This outcome suggests that the quality of the surface is strongly affected by the amount of remelting and surface leveling achieved between adjoining clad tracks. An increase in overlap ratio produces better fusion between tracks and smaller inter-track valleys, leading to decreased surface roughness of the coating. On the other hand, a higher overlap could lead to excessive heat accumulation and molten pool instability, which can cause geometrical irregularities on the surface of the coating [21, 22].

The scanning speed (X_2) was identified as the second most influential linear factor, with an F-value of 23.58 ($p < 0.001$). As scanning speed is known to control the interaction time of the laser beam with the material, it can influence thermal history, solidification, and melt pool stability during processing. The powder feed rate (X_3) also had a significant effect on surface roughness ($F = 11.31$, $p = 0.003$). A higher powder feed rate might cause more powder to be supplied than can be melted in the molten pool, leaving partially melted particles that lead to local accumulation of material and higher surface roughness [22-25].

In contrast, the linear effect of laser power (X_1) was not statistically significant ($F = 1.02$, $p = 0.327$). However, due to the significance of its quadratic term, laser power still has an influence on the surface morphology through nonlinear thermal effects. Too low energy input may lead to incomplete melting, while too much energy input may cause spattering, molten pool oscillation and thermal instability, which can result in roughness increase.

The quadratic terms further revealed the nonlinear nature of roughness formation. Among them, X_4^2 exhibited the highest F-value (111.77, $p < 0.001$), followed by X_1^2 ($F = 74.46$, $p < 0.001$) and X_3^2 ($F = 71.67$, $p < 0.001$). These results confirm that the influence of overlap ratio, laser power, and powder feed rate cannot be adequately described by linear relationships alone. Conversely, the quadratic term X_2^2 was statistically insignificant ($F = 0.93$, $p = 0.347$), indicating that the effect of scanning speed remained predominantly linear within the investigated parameter range.

Based on the ANOVA results, the overlap ratio was the most influential factor for the surface roughness of laser-cladded Stellite 6 coatings, while scanning speed and powder feed rate also significantly affected the roughness response. Moreover, significant quadratic terms indicated that surface roughness formation during laser cladding exhibited strong nonlinear characteristics caused by heat accumulation, remelting mechanism, and molten pool behaviors.

3.4. Main Effects of Process Parameters on Surface Roughness

Figure 4 presents the main effects plot of laser Power (P), Scanning Speed (Vs), Powder Feed Rate (Mp), and Overlap Ratio (O) on the surface roughness Rz of the laser-cladded Stellite 6 coatings. Each point represents the average Rz value obtained at the corresponding factor level.

The main effects plot indicates that the slope of each curve reflects the relative influence of the corresponding parameter on surface roughness. Among the investigated factors, the overlap ratio exhibited the steepest slope, indicating that it had the most pronounced effect on Rz, which is consistent with the ANOVA results.

For laser power, the average Rz increased significantly when the power was raised from 1800 to 2000 W and then decreased at 2200 W. The observed trend is consistent with the fact that moderate power levels may promote molten pool instability, whereas higher power improves powder melting and remelting between adjacent tracks, resulting in a smoother surface.

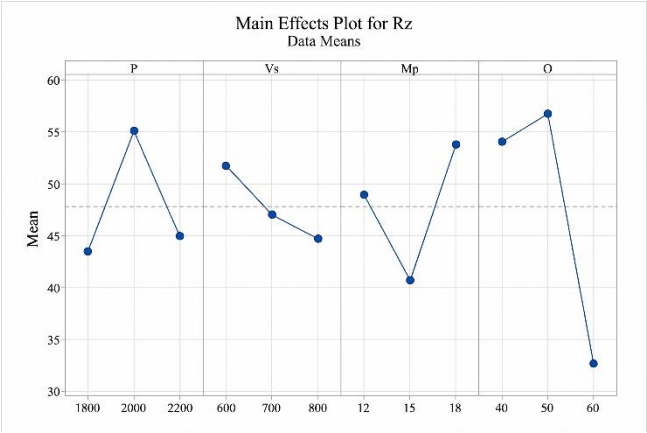

Fig. 4 Main effects plot of laser cladding parameters on the surface roughness

The scanning speed showed a relatively weak effect on surface roughness. Increasing the scanning speed from 600 to 800 mm/min led to a gradual decrease in Rz. This trend can be attributed to reduced heat accumulation and improved solidification stability at higher travel speeds.

The powder feed rate had a pronounced nonlinear effect. The lowest average Rz was obtained at 15 g/min, while both lower and higher feed rates resulted in increased roughness.

At excessive feed rates, the supplied powder may exceed the melting capacity of the laser, causing partially melted particles and irregular surface features.

The overlap ratio was the most influential parameter. Increasing the overlap ratio from 40% to 60% resulted in a substantial reduction in surface roughness, with the lowest mean Rz observed at 60% overlap.

This improvement is attributed to enhanced remelting and surface leveling between neighboring clad tracks, which effectively reduces inter-track valleys and peak irregularities [23-25].

Based on the main effects plot, the combination of P = 1800 W, Vs = 800 mm/min, Mp = 15 g/min, and O = 60% is expected to provide the lowest surface roughness within the investigated range. These findings confirm that optimizing the overlap ratio and laser power is essential for achieving a high-quality surface finish, thereby reducing post-machining allowance and improving the dimensional quality of laser-cladded cylindrical shafts.

3.5. Interaction Effects of Process Parameters

The interaction plot shown in Figure 5 reveals that several parameter combinations produced non-parallel and intersecting curves, indicating significant interactions among the investigated factors.

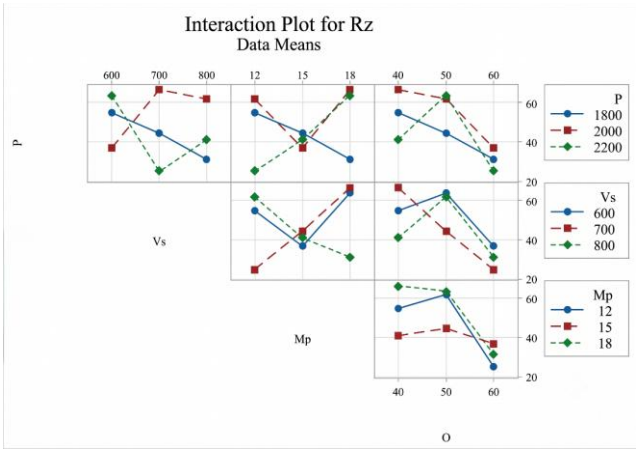

Fig. 5 Interaction effects of laser cladding parameters on the surface roughness Rz of Stellite 6 coatings

Strong interactions were observed between laser power and scanning speed, laser power and powder feed rate, and laser power and overlap ratio. These results demonstrate that the effect of one parameter depends on the level of the others.

In particular, the beneficial effect of a high overlap ratio was more pronounced at elevated laser power. At 1800 W and 60% overlap, the remelting between neighboring tracks was sufficient to eliminate inter-track valleys and produce the smoothest coating surface. The strong interaction between laser power and overlap ratio demonstrates that effective remelting requires both sufficient energy input and appropriate track superposition. The interaction between laser power and scanning speed reflects the combined effect of energy density and interaction time on molten pool stability [22-25].

Overall, the interaction plots indicate that surface roughness is governed by the combined effects of heat input, powder supply, and overlap ratio rather than by any single parameter.

3.6. Regression Model Development and Evaluation

A second-order regression model was developed using Minitab to predict the surface roughness Rz as a function of the four process parameters:

$$R_z = 55.98 + 0.732X_1 - 3.526X_2 + 2.443X_3 - 10.670X_4 - 10.85X_1^2 + 1.21X_2^2 + 10.65X_3^2 - 13.30X_4^2$$

Coefficients

Term	Coef	SE Coef	T-Value	P-Value	VIF
Constant	55,98	1,78	31,47	0,000	
X1	0,732	0,726	1,01	0,327	1,00
X2	-3,526	0,726	-4,86	0,000	1,00
X3	2,443	0,726	3,36	0,003	1,00
X4	-10,670	0,726	-14,69	0,000	1,00
X1*X1	-10,85	1,26	-8,63	0,000	1,00
X2*X2	1,21	1,26	0,97	0,347	1,00
X3*X3	10,65	1,26	8,47	0,000	1,00
X4*X4	-13,30	1,26	-10,57	0,000	1,00

Model Summary

S	R-sq	R-sq(adj)	R-sq(pred)
3,08098	96,59%	95,08%	92,34%

Fig. 6 Results of regression model analysis

The regression coefficients and their statistical significance are summarized in Figure 6. The developed second-order regression model was established using the coded variables X_1, X_2, X_3, and X_4, representing laser power, scanning speed, powder feed rate, and overlap ratio, respectively. The analysis shows that the linear terms X_2, X_3, and X_4, as well as the quadratic terms X_1^2, X_3^2, and X_4^2, were statistically significant ($p < 0.05$). In contrast, the linear term X_1 ($p = 0.327$) and the quadratic term X_2^2 ($p = 0.347$) were not statistically significant within the investigated parameter range.

Among the linear effects, the overlap ratio (X_4) exhibited the largest absolute T-value (|T| = 14.69), indicating that it was the most influential parameter affecting surface roughness. The negative coefficient of X_4 (-10.670) suggests that increasing the overlap ratio significantly reduces the Rz value by enhancing remelting and surface leveling between adjacent clad tracks. This observation is consistent with the ANOVA results and previous studies on laser cladding surface formation.

The scanning speed (X_2) also showed a significant negative effect (T = -4.86, $p < 0.001$), indicating that higher scanning speeds tend to reduce surface roughness by limiting excessive heat accumulation and promoting more stable solidification conditions. Conversely, the positive coefficient of the powder feed rate (X_3 = +2.443) indicates that increasing powder supply may increase roughness due to incomplete melting and local material accumulation when the powder input exceeds the melting capacity of the molten pool.

The quadratic terms further confirm the nonlinear nature of surface roughness formation. The largest nonlinear contribution was associated with X_4^2 (T = -10.57, $p < 0.001$), followed by X_1^2 (T = -8.63, $p < 0.001$) and X_3^2 (T = 8.47, $p < 0.001$). The analysis shows that overlap ratio, laser power, and powder feed rate possess optimal operating ranges beyond which the surface quality deteriorates. In contrast, the quadratic term X_2^2 was statistically insignificant, suggesting that the effect of scanning speed remained predominantly linear within the investigated range.

The regression model exhibited a high coefficient of determination (R^2 = 96.59%), together with an adjusted R^2 of 95.08% and a predicted R^2 of 92.34%. The close agreement among these values indicates that the developed model provides an excellent fit to the experimental data and possesses good predictive capability within the investigated parameter range.

In general, the regression analysis verified that the developed second-order model adequately captures the nonlinear relationship between surface roughness and laser cladding parameters. Also, the proposed model is statistically sound and agrees well with the physics-based explanation of molten pool formation, remelting, and heat accumulation phenomena. Thus, the model can therefore serve as a useful tool for selecting processing parameters that achieve lower surface roughness, thereby reducing post-machining allowance and improving the dimensional quality of laser-cladded shaft components. Referring to the developed quadratic regression equation and main effects plot, the following set of processing parameters was found to produce minimum surface roughness on Stellite 6 coating: laser power - 1800 W, scanning speed - 800 mm/min, powder feed rate - 15 g/min, and overlap ratio - 60%. Among all input factors studied in this work, the overlap ratio had the strongest effect on the Rz response. Improved remelting by increasing the overlap ratio to 60% enabled better leveling of the laser-clad surface between adjacent clad tracks, which reduced inter-track valleys and leveled out the coating surface. High scanning speed also played an important role in achieving low surface roughness by reducing excessive heat accumulation and leading to more consistent solidification conditions. In addition, intermediate powder feed rate led to balanced feeding of powder particles into the molten pool and reduced exposure of unmelted particles on the cladded surface due to a better match between powder feeding rate and molten pool melting capacity [22-25]. Although laser power had only a moderate linear effect on Rz, its nonlinear effect was still significant. As such, a lower laser power level of 1800 W was chosen because it was more conducive to achieving minimum Rz values within the constrained parameter space. According to the regression model, these processing conditions should result in a minimum average surface roughness of 18.11 μm.

As stated earlier, the purpose of conducting the confirmation experiment is to determine the accuracy of the developed reduced quadratic regression model. In this experiment, the chosen factor levels were selected based on the prediction from the regression analysis and the main effects plot. This combination corresponds to a laser power of 1800 W, scanning speed of 800 mm/min, powder feed rate of 15 g/min, and overlap ratio of 60%. According to the prediction from the regression model, the resulting surface roughness should be around 18.11 μm for these parameters. Afterwards, the confirmation experiment was carried out with these processing parameters, and the resulting average Rz was found to be 19.55 μm. The percent relative error between prediction and experimental value is calculated as:

$$\text{Error} = \frac{|Rz_{exp} - Rz_{pred}|}{Rz_{exp}} \times 100$$

The calculated prediction error was 7.4%, which is lower than 10%, indicating good agreement between the regression model and the experimental results. This confirms that the developed model can reliably predict the surface roughness within the investigated parameter range and can be effectively used for process parameter optimization in laser cladding of Stellite 6 coatings on cylindrical AISI 1045 steel shafts.

4. Conclusion

In this work, the influence of laser Power (P), Scanning Speed (Vs), Powder Feed Rate (Mp), and Overlap Ratio (O) on Surface Roughness (Rz) during laser cladding of Stellite 6 coatings on cylindrical shafts made of AISI 1045 steel substrate was investigated using Taguchi L9 design. The obtained results revealed that average surface roughness ranged from 30.09 to 66.44 μm, considering the tested range of process parameters. Statistical analysis proved that among the studied parameters, overlap ratio had the greatest influence

on surface roughness, while scanning speed and powder feed rate had the next strongest impact. The improvement of surface quality is achieved by the increase of the overlap ratio due to higher remelting and leveling of adjacent clad tracks.

Moreover, ANOVA showed that the developed quadratic regression model was statistically significant ($F = 63.83$, $p < 0.001$). The findings also indicate that the nonlinear relationship between the evaluated process parameters and response exists and is especially strong for overlap ratio, laser power, and powder feed rate.

Predictions using the developed model describe experimental roughness response properly and can be helpful for optimization purposes. Analysis of the regression model coefficients and plotting the main effects revealed that optimal values of laser power, scanning speed, powder feed rate, and overlap ratio to obtain minimal surface roughness are 1800 W, 800 mm/min, 15 g/min, and 60%, respectively. When applying these parameter values, the predicted average surface roughness is equal to 18.11 μm. The confirmation test was executed at the predicted optimum condition. The experimental average surface roughness achieved at this point was 19.55 μm. The difference between the predicted and experimental value was only 7.4%, which is a good agreement. These results confirm that the developed regression model can be reliably used for optimization. The proposed parameter combination provides a practical reference for reducing surface roughness and post-machining allowance in laser-clad shaft components.

References

[1] William M. Steen, and Jyotirmoy Mazumder, *Laser Material Processing*, 4th ed., Springer, 2010. [CrossRef] [Google Scholar] [Publisher Link]

[2] Joseph R. Davis, *ASM Specialty Handbook: Nickel, Cobalt, and Their Alloys*, ASM International, pp. 1-442, 2000. [Google Scholar] [Publisher Link]

[3] Ehsan Toyserkani, Amir Khajepour, and Stephen F. Corbin, *Laser Cladding*, Boca Raton, CRC Press, pp. 1-280, 2004. [CrossRef] [Google Scholar] [Publisher Link]

[4] Yanan Liu et al., "Research and Progress of Laser Cladding on Engineering Alloys: A Review," *Journal of Manufacturing Processes*, vol. 66, pp. 341-363, 2021. [CrossRef] [Google Scholar] [Publisher Link]

[5] Andrew J. Pinkerton, "Advances in the Modeling of Laser Direct Metal Deposition," *Journal of Laser Applications*, vol. 27, pp. 1-8, 2015. [CrossRef] [Google Scholar] [Publisher Link]

[6] Anish Nair, and Adam Khan M, "Studies on Effect of Laser Processed Stellite 6 Material and its Electrochemical Behavior," *Optik*, vol. 220, 2020. [CrossRef] [Google Scholar] [Publisher Link]

[7] C. Navas et al., "Tribological Properties of Laser Clad Stellite 6 Coatings on Steel Substrates," *Surface Engineering*, vol. 22, no. 1, pp. 26-34, 2006. [CrossRef] [Google Scholar] [Publisher Link]

[8] Maximilian Kiehl et al., "Coaxial Laser Cladding of Cobalt-Base Alloy Stellite™ 6 on Grey Cast Iron Analysis of the Microstructural and Mechanical Properties Depending on the Laser Power," *Journal of Materials Engineering and Performance*, vol. 32, pp. 3821-3838, 2023. [CrossRef] [Google Scholar] [Publisher Link]

[9] V. Ocelík et al., "On the Geometry of Coating Layers Formed by Overlap," *Surface and Coatings Technology*, vol. 242, pp. 54-61, 2014. [CrossRef] [Google Scholar] [Publisher Link]

[10] Changrong Chen et al., "Simplification and Experimental Investigation of Geometrical Surface Smoothness Model for Multi-Track Laser Cladding Processes," *Journal of Manufacturing Processes*, vol. 36, pp. 621-628, 2018. [CrossRef] [Google Scholar] [Publisher Link]

[11] D. Tanigawa et al., "Effect of Laser Path Overlap on Surface Roughness and Hardness of Layer in Laser Cladding," *Science and Technology of Welding and Joining*, vol. 20, no. 7, pp. 601-606, 2015. [CrossRef] [Google Scholar] [Publisher Link]

[12] Parvaneh Zareh, and R. J. Urbanic, "Experimental Analysis of Single Layer Multi-Track Deposition of Clad Beads with Variable Overlap Percentages," *The International Journal of Advanced Manufacturing Technology*, vol. 109, pp. 1511-1525, 2020. [CrossRef] [Google Scholar] [Publisher Link]

[13] Fengyuan Shu et al., "Microstructure and Mechanical Properties of Two-Layer Laser-Cladded Co-Based Coatings," *Journal of Thermal Spray Technology*, vol. 28, pp. 1330-1338, 2019. [CrossRef] [Google Scholar] [Publisher Link]

[14] Kaiming Wang et al., "Effect of Cobalt on Microstructure and Wear Resistance of Ni-Based Alloy Coating Fabricated by Laser Cladding," *Metals*, vol. 7, no. 12, pp. 1-12, 2017. [CrossRef] [Google Scholar] [Publisher Link]

[15] Xiaobin Liu et al., "Tribological Behaviors of High-Hardness Co-Based Amorphous Coatings Fabricated by Laser Cladding," *Tribology International*, vol. 162, 2021. [CrossRef] [Google Scholar] [Publisher Link]

[16] Fathollah Hosseinali Sani, Ali Reza Ebrahimi, and Hossein Jamali, "Evaluation of Microstructure and Wear Behavior of Laser-Clad Stellite 6 on AISI 5046 Steel," *Materials Today Communications*, vol. 52, pp. 1-18, 2026. [CrossRef] [Google Scholar] [Publisher Link]

[17] Ziyi Yang et al., "Microstructure, Hardness and Slurry Erosion-Wear Behaviors of High-Speed Laser Cladding Stellite 6 Coatings Prepared by the Inside-Beam Powder Feeding Method," *Journal of Materials Research and Technology*, vol. 19, pp. 2596-2610, 2022. [CrossRef] [Google Scholar] [Publisher Link]

[18] Thang Le Toan, and Nguyen Van Cuong, "Evaluation of the Mechanical Properties and the Corrosion Resistance of the Cobalt-Base Alloy Stellite 6 on 1045 Steel by Laser Cladding," *Engineering, Technology & Applied Science Research*, vol. 15, no. 3, pp. 23323-23329, 2025. [CrossRef] [Google Scholar] [Publisher Link]

[19] B46.1 - *Surface Texture (Surface Roughness, Waviness, and Lay)*, American Society of Mechanical Engineers, New York, USA, 2019. [Google Scholar] [Publisher Link]

[20] ISO 4287:1997, *Geometrical Product Specifications—Surface Texture: Profile Method—Terms, Definitions and Surface Texture Parameters*. Geneva, Switzerland: International Organization for Standardization, 1997. [Google Scholar] [Publisher Link]

[21] Luan Zhang et al., "Influence of Laser Power on Microstructure and Properties of Laser Clad Co-based Amorphous Composite Coatings," *Surfaces and Interfaces*, vol. 6, pp. 18-23, 2017. [CrossRef] [Google Scholar] [Publisher Link]

[22] Andrew J. Pinkerton, and Lin Li, "Modelling the Geometry of a Moving Laser Melt Pool and Deposition Track via Energy and Mass Balances," *Journal of Physics D: Applied Physics*, vol. 37, no. 14, pp. 1885-1895, 2004. [CrossRef] [Google Scholar] [Publisher Link]

[23] Hakan Aydin, Adem Karşi, and Meryem Altay, "Effect of Overlap Rate on the Properties of a Martensitic Stainless Steel Laser Cladding onto Ductile Cast Iron," *International Journal of Metalcasting*, vol. 20, pp. 520-531, 2026. [CrossRef] [Google Scholar] [Publisher Link]

[24] T. DebRoy et al., "Additive Manufacturing of Metallic Components – Process, Structure and Properties," *Progress in Materials Science*, vol. 92, pp. 112-224, 2018. [CrossRef] [Google Scholar] [Publisher Link]

[25] Pasquale Cavaliere, *Laser Cladding of Metals*, Springer, 2021. [CrossRef] [Google Scholar] [Publisher Link]